

ORIGINAL ARTICLE

# Spatiotemporal prediction of fine particulate matter using high-resolution satellite images in the Southeastern US 2003–2011

Mihye Lee<sup>1</sup>, Itai Kloog<sup>2</sup>, Alexandra Chudnovsky<sup>3</sup>, Alexei Lyapustin<sup>4</sup>, Yujie Wang<sup>5</sup>, Steven Melly<sup>6</sup>, Brent Coull<sup>7</sup>, Petros Koutrakis<sup>1</sup> and Joel Schwartz<sup>1</sup>

Numerous studies have demonstrated that fine particulate matter (PM<sub>2.5</sub>, particles smaller than 2.5 μm in aerodynamic diameter) is associated with adverse health outcomes. The use of ground monitoring stations of PM<sub>2.5</sub> to assess personal exposure, however, induces measurement error. Land-use regression provides spatially resolved predictions but land-use terms do not vary temporally. Meanwhile, the advent of satellite-retrieved aerosol optical depth (AOD) products have made possible to predict the spatial and temporal patterns of PM<sub>2.5</sub> exposures. In this paper, we used AOD data with other PM<sub>2.5</sub> variables, such as meteorological variables, land-use regression, and spatial smoothing to predict daily concentrations of PM<sub>2.5</sub> at a 1-km<sup>2</sup> resolution of the Southeastern United States including the seven states of Georgia, North Carolina, South Carolina, Alabama, Tennessee, Mississippi, and Florida for the years from 2003 to 2011. We divided the study area into three regions and applied separate mixed-effect models to calibrate AOD using ground PM<sub>2.5</sub> measurements and other spatiotemporal predictors. Using 10-fold cross-validation, we obtained out of sample R<sup>2</sup> values of 0.77, 0.81, and 0.70 with the square root of the mean squared prediction errors of 2.89, 2.51, and 2.82 μg/m<sup>3</sup> for regions 1, 2, and 3, respectively. The slopes of the relationships between predicted PM<sub>2.5</sub> and held out measurements were approximately 1 indicating no bias between the observed and modeled PM<sub>2.5</sub> concentrations. Predictions can be used in epidemiological studies investigating the effects of both acute and chronic exposures to PM<sub>2.5</sub>. Our model results will also extend the existing studies on PM<sub>2.5</sub> which have mostly focused on urban areas because of the paucity of monitors in rural areas.

*Journal of Exposure Science and Environmental Epidemiology* advance online publication, 17 June 2015; doi:10.1038/jes.2015.41

**Keywords:** empirical/statistical models; exposure modeling; particulate matter; personal exposure

## INTRODUCTION

Since the Six Cities study,<sup>1</sup> which showed a strong linear relationship between PM<sub>2.5</sub> and mortality between cities that differed by pollution level, a body of literature has reported effects of PM<sub>2.5</sub> on mortality and morbidity.<sup>2–4</sup> In many of those studies, the PM<sub>2.5</sub> exposures were assessed by using concentration data obtained at a central monitoring site located in a jurisdiction or within a specified distance. However, this approach introduces information bias, and thus leads to attenuation of the magnitude of effects of air pollution or increases the variance of estimate.<sup>5–7</sup> Many studies have attempted to address this issue and to produce PM<sub>2.5</sub> concentrations for locations distant from the monitors.<sup>8–10</sup> This includes predicting PM<sub>2.5</sub> levels using regression models based on geographic covariates such as land-use regressions or geostatistical interpolation methods such as Kriging.<sup>8,11,12</sup> However, predictions from a land-use regression are limited to long-term exposures for chronic health effects studies, since the geographic covariates are mostly not time varying.<sup>13</sup> Moreover, if the amount of pollution due to a geographic predictor, for example, traffic density, changes over time because of control

technology, this is not easily incorporated into land-use regression. Geostatistical methods also have limitations because of the low density of monitoring stations, rendering the results unreliable especially in rural areas. Meanwhile, the aerosol optical depth (AOD) values from the Moderate-Resolution Imaging Spectroradiometer (MODIS) satellite provide daily measurements for the entire earth. AOD is a measure of particles in a column of air and is related to PM<sub>2.5</sub>.<sup>14</sup> With the advent of a new processing algorithm called Multi-Angle Implementation of Atmospheric Correction (MAIAC),<sup>15</sup> the spatial resolution of AOD has further improved from 10 × 10 km<sup>2</sup> to 1 × 1 km<sup>2</sup>. Since the relationship between the AOD measurement and PM<sub>2.5</sub> is affected by various factors such as the optical properties of particulates, mixing height, and humidity, which vary daily, we used a mixed-effect model with daily random slopes for daily calibration rather than a general regression. This provides better predictive performance than other studies using the satellite imagery for the PM<sub>2.5</sub> prediction without daily calibration.<sup>16</sup>

In this paper, we used AOD satellite data and predictors such as meteorological variables, land-use regression, and spatial

<sup>1</sup>Exposure, Epidemiology, and Risk Program, Department of Environmental Health, Harvard School of Public Health, Boston, Massachusetts, USA; <sup>2</sup>Department of Geography and Environmental Development, Ben-Gurion University of the Negev, Beer Sheva, Israel; <sup>3</sup>Department of Geography and Human Environment, Tel-Aviv University, Israel; <sup>4</sup>GEST/UMBC, NASA Goddard Space Flight Center, Baltimore, Maryland, USA; <sup>5</sup>University of Maryland Baltimore County, Baltimore, Maryland, USA; <sup>6</sup>Department of Epidemiology and Biostatistics, Drexel University School of Public Health, Philadelphia, Pennsylvania, USA and <sup>7</sup>Department of Biostatistics, Harvard School of Public Health, Boston, Massachusetts, USA. Correspondence: Dr. Mihye Lee, Exposure, Epidemiology and Risk Program, Department of Environmental Health, Harvard School of Public Health, Boston, MA, USA. Tel.: 617 998 1027. Fax: 617 384 8745.

E-mail: mil724@mail.harvard.edu

Received 8 January 2015; revised 8 April 2015; accepted 27 April 2015

smoothing to predict the daily concentration of PM<sub>2.5</sub> at a 1-km<sup>2</sup> resolution across the Southeastern United States, including seven states of Georgia, North Carolina, South Carolina, Alabama, Tennessee, Mississippi, and Florida for the years 2003 to 2011.

## DATA

### Ground Particulate Matter Measurements

We obtained PM<sub>2.5</sub> mass concentration data from Federal Reference Method monitors operated by the US Environmental Protection Agency (EPA) and monitors with a teflon filter in the Interagency Monitoring of Protected Visual Environments program for a total of 257 monitoring sites.

### Aerosol Optical Depth Data

The MAIAC data were obtained from the National Aeronautics and Space Administration (NASA) at the resolution of 1 km<sup>2</sup>. AOD data were delivered by tiles, which is the unit of spatial domain of MODIS image with an area of 10 × 10° at the equator. Our study used tiles h00v03, h01v02, h01v03, h01v04, h02v02, and h02v03. The data include the latitude and longitude in the WGS84 coordinate system, the corresponding AOD values, and a quality flag. We deleted AOD values higher than 1.5 likely reflecting cloud contamination and AOD values over water bodies since the water reflects light and affects the reliability of AOD readings. The AOD value which was the closest in distance within a 1-km buffer was assigned to each PM<sub>2.5</sub> measurement.

To compare the new MAIAC data at a 1-km<sup>2</sup> resolution with the existing data at a 10-km<sup>2</sup> resolution, we decided to use the existing AOD data that we had retained. For the years 2000–2010, MODIS level 2 files from the Earth Observing System Terra satellite were used to extract AOD values at a 10 km × 10-km resolution.

### Meteorological Data

We downloaded weather data from the National Climatic Data Center (NCDC, 2010) website. Weather variables include temperature, relative humidity, wind speed, visibility, and sea level pressure in the form of the daily mean. A total of 144 weather stations were used and we assigned the weather readings based on the closest distance on a specific data.

### Normalized Difference Vegetation Index

NASA provides normalized difference vegetation index (NDVI) data from the MODIS sensor. We aggregated NDVI measurements to a 1-km grid and a 1-month average. Specifically we used the Terra satellite product ID of MOD13A3.

### Height of Planetary Boundary Layer

We obtained the daily height of planetary boundary layer (PBL) from the National Oceanic and Atmospheric Administration (NOAA) Reanalysis Data. The pixel resolution of PBL data was 32 × 32 km on a daily basis. To represent the daily PBL height, the 24-h mean was used.

### Land Use Variables

Emissions of PM<sub>2.5</sub>, PM<sub>10</sub>, and NO<sub>x</sub> from point sources and county area level emissions, were downloaded from National Emission Inventory (NEI) data for 2005 from the website of the environmental protection agency (EPA 2005 NEI). To produce the percentage of urbanism for each satellite grid cell at 1-km<sup>2</sup> resolution, we used the national land cover database for 2011 (NLCD 2011) data at 30-m resolution.<sup>17</sup> We reclassified land cover codes 22 (developed, low intensity), 23 (developed, medium intensity), and 24 (developed, high intensity) to 1 as an urban cell and assigned 0 for the rest of codes. The mean of binary values was

calculated for each 1-km grid cell. For the location of geographical predictors such as roads, major buildings, ports, airports, and water bodies, spatial data from ESRI Data & Maps 2004 were used (ArcGIS and ArcMap by Esri, Copyright Esri).

## METHODS

### Date Preparation

For each day, we assigned the closest AOD readings within a 1-km buffer of PM monitors. We confined our analysis to PM<sub>2.5</sub> < 80 μg/m<sup>3</sup> to eliminate influential outliers (25 observations among the total of 260,476 PM<sub>2.5</sub> measurements for 9 years). We also restricted our analysis to cells greater or equal in population to 10, since the Southeastern US includes less populated areas. AOD values > 0.5 which corresponded to PM<sub>2.5</sub> < 10 μg/m<sup>3</sup> were removed because it is likely they are because of cloud contamination. Data with AOD < 0.15 and PM<sub>2.5</sub> > 25 μg/m<sup>3</sup> were removed because we decided it is likely on those days that low PBL moved particles closer to ground level, deteriorating the relationship between AOD and ground-level PM<sub>2.5</sub> measurements.

The aim of our model lies in high-performance prediction, not associational inference between the exposure and outcome such as in the epidemiological studies. Hence, our strategy was to eliminate observations with high residuals over 10 μg/m<sup>3</sup> as too likely to distort our predictions for most observations, and to choose a model based on maximizing cross-validated (CV) *R*<sup>2</sup>. AOD values are not missing at random (for example there are more missing in the winter) which can distort the predictions. Thus, we used inverse probability weighting to account for this selection bias. Finally, the calibration between AOD and PM<sub>2.5</sub> can vary spatially, and daily. The daily variation is because of changes in particle size distribution, color, and vertical profile, and we address this by daily calibration and by using PBL data in the model using mixed-effect models with the random intercept and slopes for day. To account for spatial differences in these daily slopes, we nested them within subregions, and to account for more permanent differences between locations, we included land-use terms in our model. Specifically, we fitted the following model:

$$E(\text{PM}_{2.5,ij}) = (\beta_0 + b_{0j} + b_{0jk}) + (\beta_1 + b_{1j} + b_{2jk})\text{AOD}_{ij} + (\beta_2 + b_{2j})\text{temp}_{ij} + \sum_{m=1}^7 \beta_{1m}X_{1mij} + \sum_{n=1}^{15} \beta_{2n}X_{2ni} + \beta_{25}\text{AOD} \times \text{PBL}, \quad (1)$$

where PM<sub>2.5,ij</sub> is the PM<sub>2.5</sub> measurements at the monitoring site *i* on day *j*. β<sub>0</sub> is the intercept for the fixed effect (the population intercept) and *b*<sub>0*j*</sub> is the overall random intercept which varies by day. *b*<sub>0*jk*</sub> is the random intercept for day nested in each subregion. Similarly, β<sub>1</sub> is the slope for the fixed effect of AOD, *b*<sub>1*j*</sub> is the overall slope for the random effect of AOD for the day, and *b*<sub>2*jk*</sub> is the random slope for each day nested in each subregion. AOD is the AOD measurement that is used for the monitoring site *i* within 1 km of the site on day *j*. β<sub>2</sub> and *b*<sub>2*j*</sub> represent the slopes for the fixed effect and the random effect of temperature, respectively. temp is the temperature that is measured by the closest weather monitor to the site *i* on day *j*. β<sub>1*m*</sub> is the slopes for the fixed effect of spatiotemporal variables. *X*<sub>1*mij*</sub> is the matrix of *m*<sup>th</sup> spatiotemporal covariates on the site *i* and day *j* other than temperature and consists of seven variables: dew point temperature; sea level pressure; visibility; wind speed; absolute humidity; NDVI in the corresponding month; and PBL. β<sub>2*n*</sub> is the slopes for the fixed effect of spatial variables. *X*<sub>2*ni*</sub> is the matrix of 15 spatial covariates for the *i*<sup>th</sup> site which includes the percent urbanicity, elevation, the density of major roads, population within 10 km diameter, PM<sub>2.5</sub> emissions at county level, PM<sub>2.5</sub> emissions from point sources, PM<sub>10</sub> emission from point sources, NO<sub>x</sub> emission from point sources, canopy surface in 2001, distance to the closest A1 roads, distance to the closest airport, distance to the closest port, distance to the closest railroad, distance to a closest road, and distance to a major building. Observations with residuals over 10 μg/m<sup>3</sup> were revisited and we determined their validity by comparing PM<sub>2.5</sub> readings from the surrounding monitors and the previous day and the next day. If we determined them to be erroneous, we assigned the readings from the closest monitoring station within 15 km.

### Model

Because of the vast study area, a single model was not able to achieve the best performance in prediction. The Southeastern US consists of various areas with different topography, climate (tropical in Florida), and

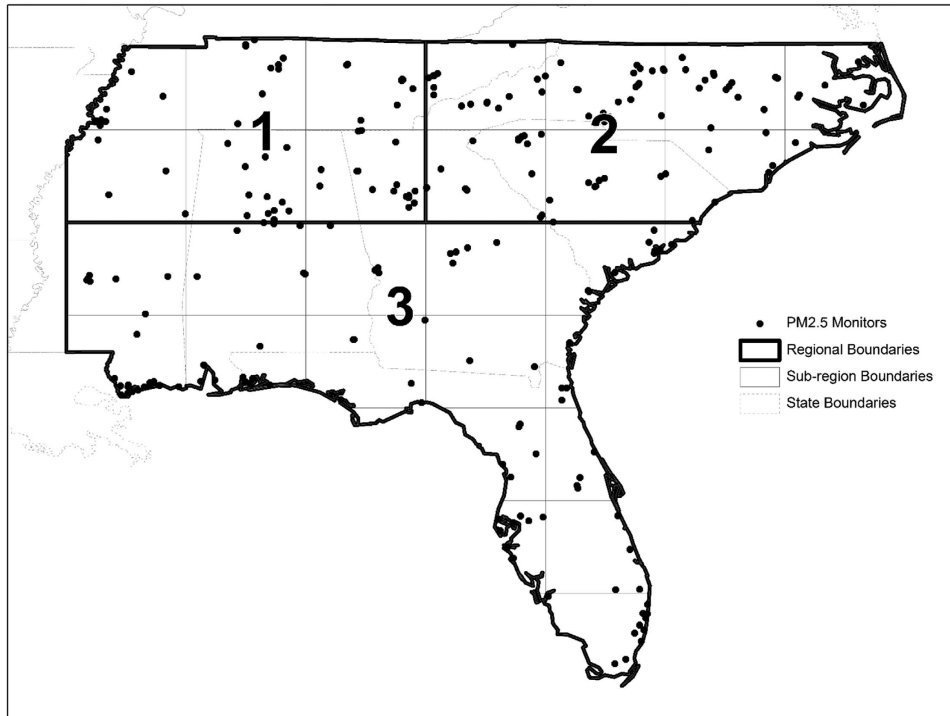


**Figure 1.** Study area and the locations of PM<sub>2.5</sub> monitoring stations.

geographic features such as swamps and forests. Therefore, we decided to split the study area into three regions and to fit separate models for each region and implement nested random coefficients for subregions within each region (Figure 1). Region 1 consist of Tennessee, Mississippi, Alabama, and Georgia. Region 2 covers North Carolina, South Carolina, and Georgia. Lastly, region 3 covers Florida, Mississippi, Alabama, Georgia, and South Carolina.

AOD measurement cannot be made because of various factors such as cloud or snow cover. We hypothesized that the cloud formation and snow cover is affected by weather conditions including temperature, wind speed, sea level pressure, elevation, and the season. Therefore, to adjust the non-random missingness of AOD, we modeled inverse probability weights (IPW) and applied them to the first stage models. Specifically, we fitted the following logistic model for the missingness of AOD measurements:

$$E(\text{logit}(p)) = \beta_0 + \beta_1 \text{temp}_{ij} + \beta_2 \text{WS}_{ij} + \beta_3 \text{SLP}_{ij} + \beta_4 \text{elev}_i + \beta_5 \text{mon}_j, \quad (2)$$

where temp is temperature of cell *i* on day *j*, WS<sub>ij</sub> is wind speed of cell *i* on day *j*, SLP<sub>ij</sub> is the sea level pressure of cell *i* on day *j*, elev is the elevation of cell *i*, and mon is the corresponding month that day *j* falls in.

Using the probability of the outcome (missing or not), we computed the inverse probability as  $\frac{1}{p}$ . Next, we normalized IPW values by dividing them by their mean. These were applied to the subsequent models as a weight.

Each of the models corresponding to the three regions was evaluated using a 10-fold cross-validation to avoid overfitting. We adopted a different approach in cross-validation which other similar studies performed record-based cross-validation. We conducted site-based cross-validation since we believed that cross-validation by monitoring stations was more appropriate, so that it assesses the capabilities of the models to predict spatial variability. Firstly, we made a randomly ordered list of monitoring stations in each region. The station list then was split into 10 subsets. In turn, 90% of the monitoring stations were used to fit the model and 10 % of stations were used to test the model performance. This cross-validation were conducted for 10 times for each region. The site-based 10-fold cross-validated  $R^2$  was used for finalizing the models rather than modeled  $R^2$  as well as for assessing the model performance and for avoiding overfitting. As a result, we ended up the following models based on the highest  $R^2$  from the 10-fold cross-validation.

In region 1, we fitted the following model for each year with the IPW:

$$E(\text{PM}_{2.5ij}) = (\beta_0 + b_{0j} + b_{0jk}) + (\beta_1 + b_{1j} + b_{1jk}) \text{AOD}_{ij} + \beta_2 \text{temp}_{ij} + \beta_3 \text{dewp}_{ij} + \beta_4 \text{slp}_{ij} + \beta_5 \text{wdsp}_{ij} + \beta_6 \text{visib}_{ij} + \beta_7 \text{ah}_{ij} + \beta_8 \text{NDVI} + \beta_9 \text{elev}_i + \beta_{10} \text{pbl}_{ij} + \beta_{11} \text{urb}_i + \beta_{12} \text{emission}_i + \beta_{13} \text{PM}_{10i} + \beta_{14} \text{NOX}_i, \quad (3)$$

where PM<sub>2.5ij</sub> is the PM<sub>2.5</sub> measurements at the monitoring site *i* on day *j*.  $\beta_0$  denotes the fixed effect intercept term (population intercept) and  $b_{0j}$  is the random effect intercept varies randomly from one day to another.  $b_{0jk}$  is the random intercept for day nested in each subregion. Similarly,  $\beta_1$  is the slope for the fixed effect of AOD,  $b_{1j}$  is the slope for the random effect of AOD for each day, and  $b_{1jk}$  is the random slope for each day nested in each subregion. AOD is the AOD measurement that is used for the monitoring site *i* within 1 km of the site on day *j*. temp is the temperature that is measured by the closest weather monitor to the site *i* on day *j*. dewp is the dew point that is measured by the closest weather monitor to the site *i* on day *j*. slp is the sea level pressure in millibars that is measured by the closest weather monitor to the site *i* on day *j*. wdsp is the wind speed in knots that is measured by the closest weather monitor to the site *i* on day *j*. visib is the visibility in miles that is measured by the closest weather monitor to the site *i* on day *j*. elev is the elevation of the site *i*. pbl is the height of the planetary boundary layer at the site *i* on day *j*. urb is the percentage of urbaness at the site *i*. emission is the annual emission of PM<sub>2.5</sub> in ton from the closest point source such as an industrial factory. PM<sub>10</sub> is the annual emission of PM<sub>10</sub> in ton from the closest point source such as an industrial factory. NOX is the annual emission of NO<sub>x</sub> in ton from the closest point source such as an industrial factory.

In region 2, we fitted the following model for each year with the IPW:

$$E(\text{PM}_{2.5ij}) = (\beta_0 + b_{0j} + b_{0jk}) + (\beta_1 + b_{1j} + b_{1jk}) \text{AOD}_{ij} + \beta_2 \text{temp}_{ij} + \beta_3 \text{dewp}_{ij} + \beta_4 \text{slp}_{ij} + \beta_5 \text{wdsp}_{ij} + \beta_6 \text{visib}_{ij} + \beta_7 \text{ah}_{ij} + \beta_8 \text{NDVI} + \beta_9 \text{elev}_i + \beta_{10} \text{pbl}_{ij} + \beta_{11} \text{urb}_i + \beta_{12} \text{emission}_i. \quad (4)$$

For the third region, we fitted the following model for each year with the IPW:

$$E(PM_{2.5j}) = (\beta_0 + b_{0j} + b_{0jk}) + (\beta_1 + b_{1j} + b_{1jk})AOD_{ij} + \beta_2 temp_{ij} + \beta_3 dewp_{ij} + \beta_4 slp_{ij} + \beta_5 wds_{ij} + \beta_6 visib_{ij} + \beta_7 ah_{ij} \quad (5)$$

Besides the overall  $R^2$  from the 10-fold cross-validation, we estimated a spatial  $R^2$  by regressing the annual mean of observed  $PM_{2.5}$  against that of predicted one for each site. To assess the precision of the predictions, root mean squared prediction error (RMSPE) was generated by taking the square root of the mean of squared prediction residuals. A temporal  $R^2$  was calculated by regressing the difference between the actual  $PM_{2.5}$  measurement on a specific day and the annual mean for each site against the equivalent for the predicted values from the model.

Once we finalized the calibration models by three regions as above, we predicted  $PM_{2.5}$  levels based on the coefficients for AOD values and other temporal and spatial variables.

For the areas and days with AOD missing, we interpolated those cells using the surrounding cells that had AOD values and thus had predictions

in the second stage. Specifically, we applied the following model with the IPW.

$$(PredPM_{2.5j}) = (\beta_0 + b_{0j} + b_{0jk}) + s(lat_i, long_i) + (\beta_1 + b_{1ik})MPM_{ij} + \beta_2 bimon_{ij} + \beta_3 pbl_{ij} + \beta_4 ah_{gm}3_{ij} + \beta_5 elev_{ij} + \beta_6 mpm \times bimon_{ij} + \beta_7 mpm \times pbl_{ij}, \quad (6)$$

where  $PredPM_{ij}$  is the predicted  $PM_{2.5}$  level at a grid cell  $i$  on a day  $j$  in stage 2.  $lat_i$  and  $long_i$  are the latitude and longitude coordinates of the cell  $i$ , respectively; and  $s()$  is a smooth function of thin plate splines.  $MPM_{ij}$  is the mean  $PM_{2.5}$  measured at monitoring stations within a 100-km buffer for the cell  $i$  on day  $j$ .

Since the purpose of the analysis of the 10-km data is to compare the performance of two data, we conducted the first stage model only. During the modeling, we applied same procedures as above with the same model with same variables, calibration, and IPW to make a fair comparison.

As for software, MATLAB 2014b was used to extract the AOD readings from the raw satellite image in the HDF format and ArcGIS Desktop 10.2.2 was used along with python scripting for data preparation. Models were implemented by using the R 3.02 and SAS 9.3 (Statistical Analysis System).

**Table 1.** Descriptive statistics of  $PM_{2.5}$  ( $\mu g/m^3$ ) and MAIAC AOD

Year	Mean PM (SD)	Mean AOD (SD)
2003	12.2 (6.5)	0.18 (0.18)
2004	12.6 (6.6)	0.18 (0.17)
2005	13.1 (7.3)	0.20 (0.19)
2006	12.6 (6.6)	0.20 (0.19)
2007	12.4 (7.5)	0.21 (0.21)
2008	10.8 (5.6)	0.18 (0.16)
2009	9.4 (4.6)	0.17 (0.15)
2010	10.2 (4.9)	0.17 (0.15)
2011	9.8 (5.3)	0.20 (0.18)

**RESULTS**

A total of 257 monitoring stations were used for the study. Figure 1 shows the study area and the locations of  $PM_{2.5}$  monitors. The study area with the thick boundary line covers most of the seven states except for the small area of Western Mississippi due to the lack of the total spatial domain consisting of AOD tiles. The numbers from 1 to 3 in big bold font indicate the study area region. Region 1 mainly consists of the states of Tennessee, and the upper part of Mississippi, Alabama, and Georgia, and contains 61 monitoring stations (0.0003 monitor/km<sup>2</sup>). Region 2 includes most of North Carolina, and major parts of South Carolina, and

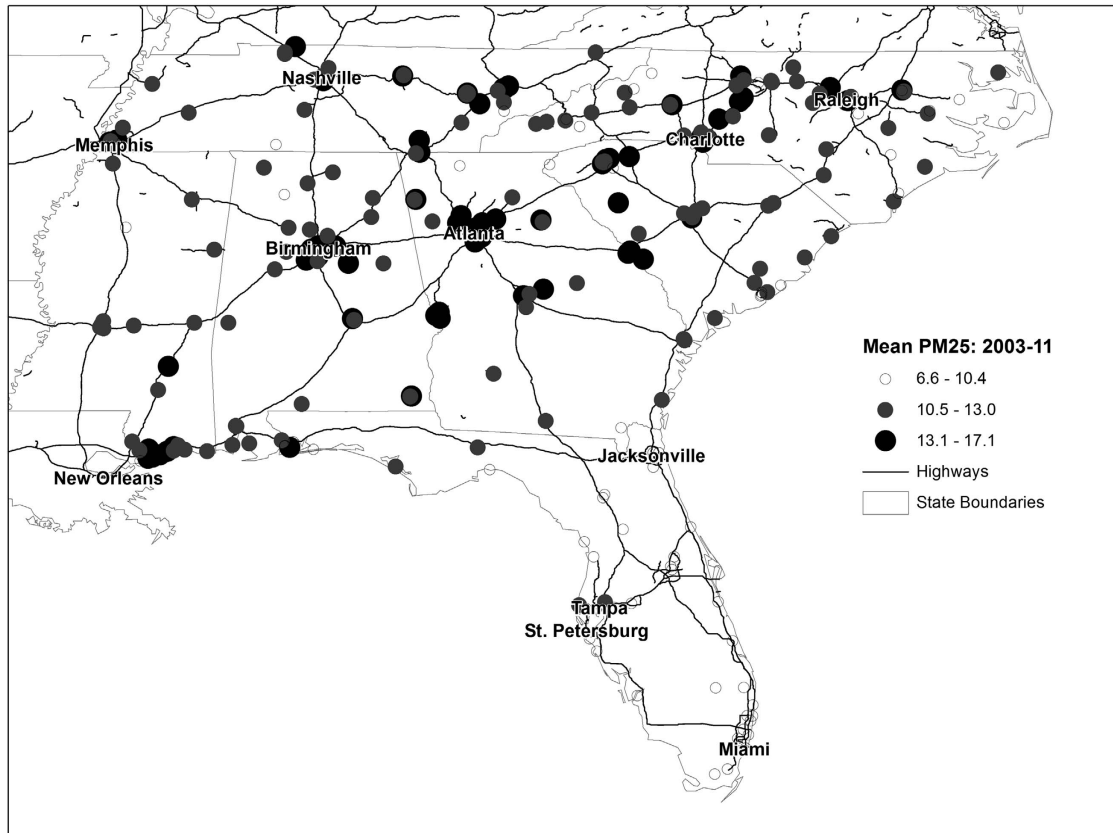


**Figure 2.** Spatial distribution of  $PM_{2.5}$  concentrations between 2003 and 2011.

**Table 2.** Result of site-based 10-fold cross-validation from stage 1 model using 1-km<sup>2</sup> data

Year	Region	R <sup>2</sup> (CV)	Slope (CV)	RMSPE (μg/m <sup>3</sup> )	Spatial R <sup>2</sup>	Temporal R <sup>2</sup>	Spatial RMSPE
2003	1	0.72	0.93	3.51	0.50	0.78	1.86
	2	0.83	0.98	2.67	0.59	0.84	1.03
	3	0.75	1.01	2.62	0.81	0.74	0.93
2004	1	0.79	0.97	2.92	0.94	0.80	1.07
	2	0.80	0.99	2.77	0.52	0.81	0.79
	3	0.74	0.99	2.83	0.77	0.74	0.86
2005	1	0.83	0.99	3.23	0.86	0.84	1.12
	2	0.80	0.97	3.12	0.81	0.81	0.93
	3	0.75	0.99	3.10	0.73	0.75	1.19
2006	1	0.80	0.98	2.99	0.53	0.83	1.26
	2	0.84	0.99	2.70	0.70	0.85	0.86
	3	0.74	1.00	2.69	0.67	0.75	1.15
2007	1	0.79	0.98	3.19	0.67	0.82	1.34
	2	0.85	0.99	2.54	0.59	0.86	0.84
	3	0.70	1.02	3.29	0.77	0.69	1.25
2008	1	0.78	0.99	2.71	0.74	0.80	0.99
	2	0.78	0.98	2.48	0.60	0.79	0.79
	3	0.69	1.00	2.74	0.85	0.65	0.99
2009	1	0.76	0.98	2.30	0.81	0.78	0.83
	2	0.78	0.99	2.05	0.81	0.79	0.78
	3	0.66	1.02	2.60	0.80	0.64	0.87
2010	1	0.65	0.95	2.80	0.33	0.71	1.33
	2	0.80	0.99	2.09	0.46	0.81	0.68
	3	0.66	1.00	2.51	0.69	0.66	1.11
2011	1	0.79	0.98	2.40	0.80	0.80	0.86
	2	0.78	0.98	2.21	0.55	0.79	0.69
	3	0.63	0.99	2.97	0.75	0.61	0.98
Mean	1	0.77	0.97	2.89	0.69	0.80	1.18
	2	0.81	0.99	2.51	0.63	0.82	0.82
	3	0.70	1.00	2.82	0.76	0.69	1.04

Georgia with 88 monitors. Region 2 is most densely populated by PM monitoring stations (0.00038 monitor/km<sup>2</sup>). Region 3 covers the most southern part, including Florida and the southern part of Mississippi, Alabama, Georgia, and South Carolina. Although region 3 has the largest number of monitors of 108, due to its vast area, the spatial distribution of PM monitoring stations is most scattered among the three regions (0.00026 monitor/km<sup>2</sup>).

Table 1 shows the descriptive statistics for PM<sub>2.5</sub> measurements from monitoring stations and AOD measurements by MAIAC algorithm in the Southeastern US by year from 2003 to 2011. The annual average of PM<sub>2.5</sub> has steadily decreased from 12.2 in 2003 to 9.8 μg/m<sup>3</sup> in 2011. The SD has also decreased from 6.5 to 5.3 μg/m<sup>3</sup>. The mean AOD readings were on the order of 0.20 (dimensionless) over 9 years.

Figure 2 shows the spatial distribution of PM<sub>2.5</sub> concentrations in the study area, represented by the average PM<sub>2.5</sub> levels by monitors during the study period (2003–2011). Monitoring stations in big cities such as Atlanta, Nashville, Charlotte, and Birmingham recorded the highest average PM<sub>2.5</sub> level. Monitors at intersections of major highways also showed the high level of PM<sub>2.5</sub>. Among the seven study states, Florida showed the lowest PM<sub>2.5</sub> level.

Our model showed a highly significant association between PM<sub>2.5</sub> and AOD after controlling for other covariates and spatiotemporal predictors. Table 2 presents results from the stage 1 model where the calibration of AOD and other spatiotemporal predictors were done by each year and region. The R<sup>2</sup> numbers are from the 10-fold cross-validation based on the sampling of monitors not observations regardless of monitors. The predictive power of the models differed by region. Region 2 showed the highest overall R<sup>2</sup> of 0.81 with the year-to-year variation ranging from 0.78 in 2008 to 0.85 in 2007. Region 3 showed the lowest

**Table 3.** R<sup>2</sup> from stage 3 model

Year	Region	R <sup>2</sup> Pred2	R <sup>2</sup> PM <sub>2.5</sub>
2003	1	0.83	0.90
	2	0.86	0.91
	3	0.61	0.85
2004	1	0.83	0.88
	2	0.84	0.90
	3	0.64	0.85
2005	1	0.83	0.91
	2	0.84	0.90
	3	0.65	0.87
2006	1	0.86	0.89
	2	0.87	0.91
	3	0.59	0.86
2007	1	0.83	0.90
	2	0.84	0.91
	3	0.62	0.88
2008	1	0.83	0.87
	2	0.82	0.88
	3	0.65	0.90
2009	1	0.81	0.86
	2	0.80	0.86
	3	0.61	0.83
2010	1	0.75	0.83
	2	0.81	0.89
	3	0.60	0.85
2011	1	0.85	0.89
	2	0.81	0.88
	3	0.61	0.87
Mean	1	0.82	0.88
	2	0.83	0.89
	3	0.62	0.86

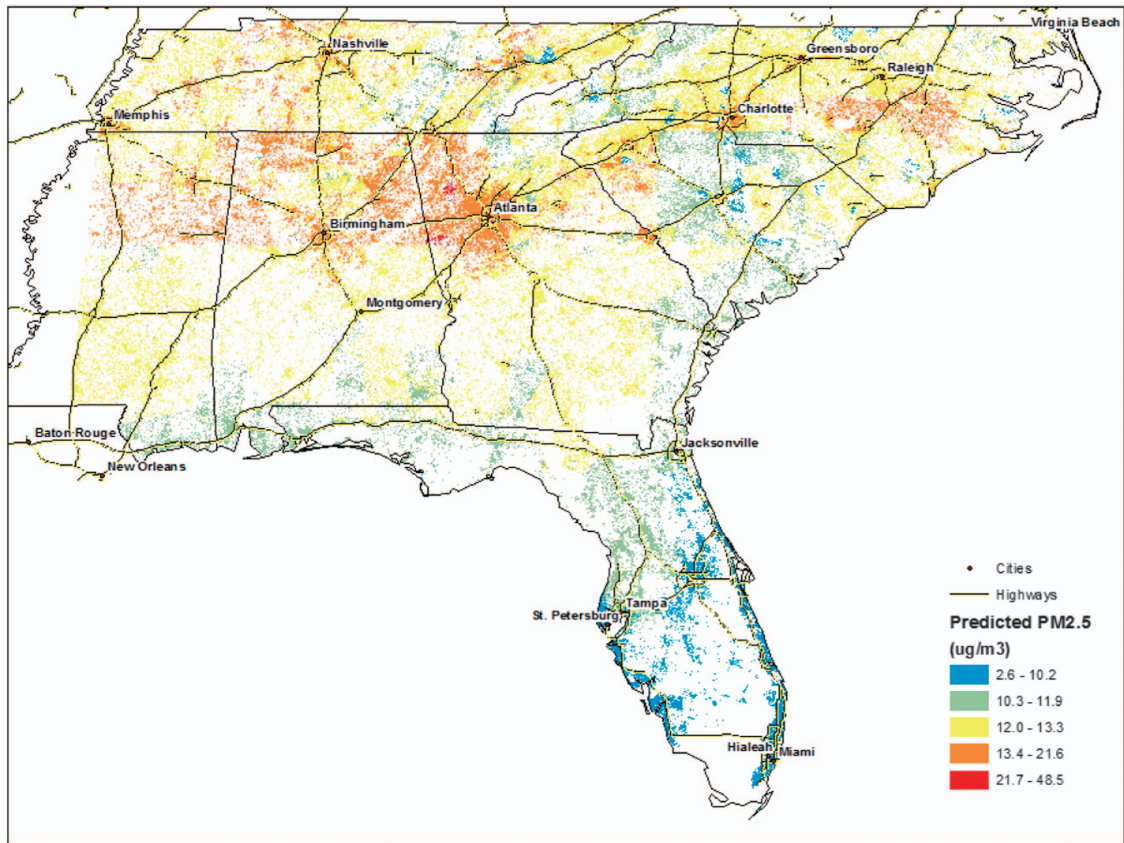


Figure 3. Predicted PM<sub>2.5</sub> level in 2003.

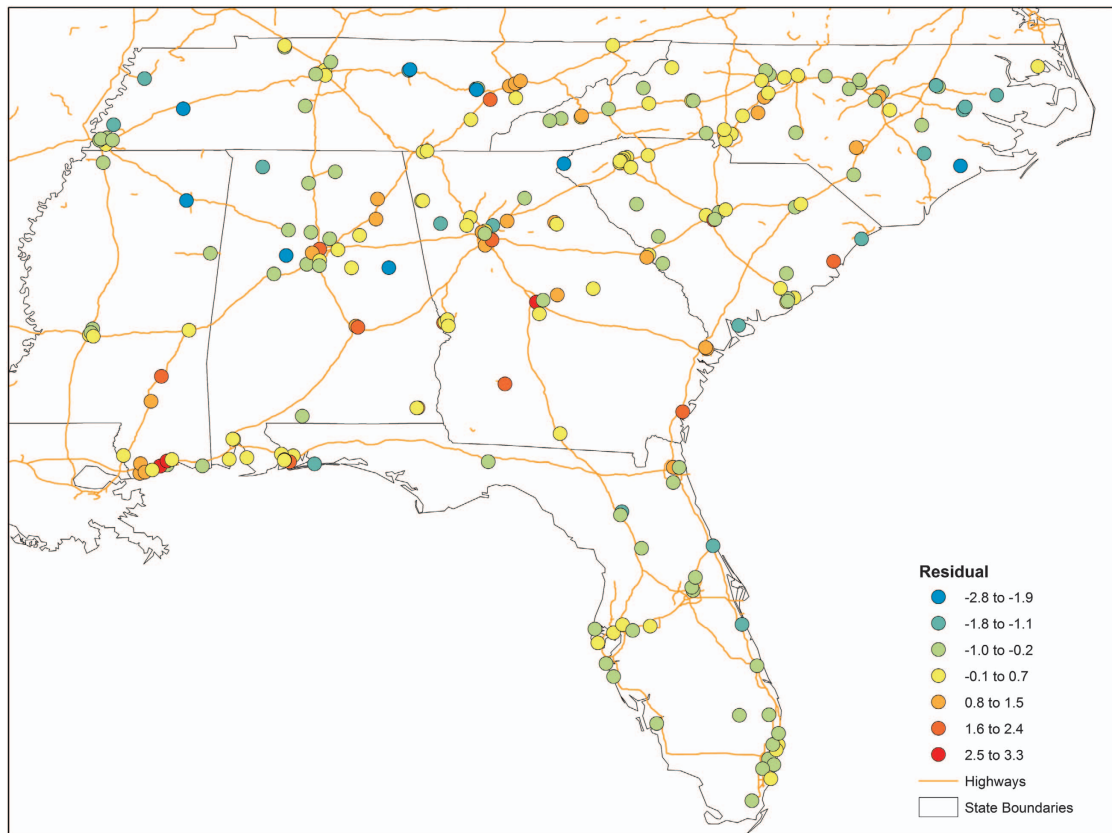


Figure 4. Residual map.

performance with an average cross-validated  $R^2$  of 0.70 (minimum of 0.63 occurred in 2011 and maximum of 0.75 occurred in 2003 and 2005). For region 1, an average cross-validated  $R^2$  was 0.77 and ranged from 0.65 in 2010 to 0.83 in 2005. The slopes between the observed PM<sub>2.5</sub> versus the modeled PM<sub>2.5</sub> were close to 1 for all the regions, suggesting a good agreement between the model results and actual measurements and the thus low bias. Region 2 exhibited the lowest average RMSPE of 2.51  $\mu\text{g}/\text{m}^3$ , followed by region 3 with 2.82  $\mu\text{g}/\text{m}^3$  and region 1 with 2.87  $\mu\text{g}/\text{m}^3$ . The RMSPE for the spatial component was much lower at 0.82  $\mu\text{g}/\text{m}^3$  in region 2. In general, the models performed better temporally than spatially. The temporal  $R^2$  values were higher than the spatial ones except for region 3. For the temporal result, the mean  $R^2$  was 0.80, 0.82, and 0.69 for regions 1, 2, and 3, respectively. For the spatial model the mean  $R^2$  was 0.69, 0.63, and 0.76 by region order.

The output prediction model based on the third model gave very similar results (Table 3). The third column represents the  $R^2$  for the prediction from stage 2 (prediction for the grid cells and days that AOD readings were available) and the last column illustrates those for the comparison with actual PM<sub>2.5</sub> observations. The final prediction showed high predictive power, from 0.89 (region 2) to 0.86 (region 3).

To graphically represent the predictions, Figure 3 displays the prediction results in the form of annual average in 2003 where reveals higher PM<sub>2.5</sub> levels for highways and the main cities. The spatial pattern of predictions matches well with the one of the

measured PM<sub>2.5</sub> represented in Figure 2. There was no systematic spatial patterns of residuals during the study period (Figure 4).

Compared with the existing AOD data at a  $10 \times 10$ -km resolution, the MAIAC data at a  $1 \times 1$ -km resolution showed the better performance (Table 4). Only except for slight decrease in the mean of 10-fold cross-validated  $R^2$  for Region 1 from 0.78 to 0.77, the MAIAC data showed the higher  $R^2$  values. Especially, the performance in Region 3 drastically improved from 0.62 to 0.70. The new data also had lower errors than the existing one. RMSPE values have decreased from 3.27 to 2.89  $\mu\text{g}/\text{m}^3$  for Region 1, from 2.90 to 2.51  $\mu\text{g}/\text{m}^3$  for Region 2, and from 3.64 to 2.82  $\mu\text{g}/\text{m}^3$  for Region 3. Other indicators such as Spatial  $R^2$  and temporal  $R^2$  have also improved when using the 1-km AOD data.

## DISCUSSION

In this paper, we predicted PM<sub>2.5</sub> levels across the Southeastern US at a 1-km resolution using the MODIS satellite imagery derived by the newly developed algorithm MAIAC. Compared to the AOD data at a 10-km resolution, the MAIAC data at a 1-km resolution showed the better performance. Furthermore, higher resolution enabled the more precise exposure assessment for PM<sub>2.5</sub> at a finer scale such as the street-level address.

These results will enable epidemiological studies to evaluate the association between PM<sub>2.5</sub> and its health effects with reduced measurement error in exposure. We also anticipate study areas may extend to rural areas in the Southeastern US, which were formerly restricted to urban areas because of the distance to

**Table 4.** Result of site-based 10-fold cross-validation from stage 1 model using 10-km<sup>2</sup> data

Year	Region	$R^2$ (CV)	Slope (CV)	RMSPE ( $\mu\text{g}/\text{m}^3$ )	Spatial $R^2$	Temporal $R^2$	Spatial RMSPE
2000	1	0.84	0.99	3.76	0.64	0.85	1.09
2000	2	0.80	0.98	3.40	0.54	0.82	1.42
2000	3	0.72	1.00	4.09	0.64	0.74	1.73
2001	1	0.78	0.98	3.68	0.43	0.80	1.55
2001	2	0.79	0.99	3.18	0.52	0.80	1.14
2001	3	0.65	0.98	3.74	0.57	0.69	1.59
2002	1	0.79	0.97	3.60	0.62	0.80	1.15
2002	2	0.77	0.99	3.14	0.36	0.79	1.14
2002	3	0.63	0.96	3.72	0.58	0.63	1.40
2003	1	0.77	0.99	3.30	0.25	0.79	1.29
2003	2	0.84	0.99	2.79	0.30	0.86	1.03
2003	3	0.60	0.96	3.56	0.52	0.61	1.54
2004	1	0.75	0.97	3.30	0.36	0.77	1.25
2004	2	0.78	0.99	3.15	0.47	0.79	0.93
2004	3	0.69	0.97	3.60	0.63	0.71	1.40
2005	1	0.82	0.98	3.59	0.38	0.84	1.33
2005	2	0.81	0.99	3.20	0.58	0.83	1.06
2005	3	0.68	0.99	3.90	0.62	0.71	1.69
2006	1	0.79	1.00	3.36	0.60	0.80	1.13
2006	2	0.82	0.99	3.03	0.46	0.83	1.08
2006	3	0.62	0.97	3.45	0.55	0.64	1.60
2007	1	0.77	0.97	3.71	0.64	0.78	1.22
2007	2	0.82	0.99	2.88	0.66	0.83	0.73
2007	3	0.59	0.98	4.31	0.57	0.59	1.67
2008	1	0.77	0.98	2.79	0.46	0.79	0.99
2008	2	0.77	0.98	2.60	0.61	0.78	0.86
2008	3	0.58	0.96	3.36	0.59	0.57	1.42
2009	1	0.77	0.99	2.33	0.63	0.78	0.80
2009	2	0.75	0.99	2.15	0.78	0.77	0.76
2009	3	0.49	1.00	3.25	0.64	0.48	1.34
2010	1	0.70	0.99	2.57	0.20	0.73	0.96
2010	2	0.75	1.00	2.38	0.53	0.76	0.77
2010	3	0.55	0.99	3.02	0.68	0.54	1.38
	1	0.78	0.98	3.27	0.47	0.79	1.16
Mean	2	0.79	0.99	2.90	0.53	0.81	0.99
	3	0.62	0.98	3.64	0.60	0.63	1.52

monitoring stations. Considering that PM<sub>2.5</sub> measurements are not always daily, our model interpolates the temporal break using the daily satellite imagery and a smoothing technique as well as spatial predictions. This approach enables epidemiological studies to examine both acute and chronic effects.

Model performance varied by region. Region 2 mainly covering North Carolina revealed the highest performance (0.81) and region 3, covering the most southern part, such as Florida, had the lowest performance (0.70). One possible explanation is that the spatial density of monitoring stations affects model. Region 2 has the most abundant monitoring stations compared with its area, whereas region 3 lacks monitoring stations for its extensive area. This appeared to affect the results by providing fewer pairs to fit the model. Another explanation may be that region 2 is relatively more urbanized compared with region 3 with more land-use factors which could be taken into account. This suggestion parallels with our experience during the analysis that the calibration model based on the highest  $R^2$  for region 2 has more land-use variables than that for region 3. Lastly, the quality of AOD from the MODIS instrument and the MAIAC algorithm should be considered. Visual analysis (data not present) by AOD swath revealed that the performance of AOD differed by tile of satellite imagery. Tile h01v02 that covers North Carolina showed the best performance, whereas tiles around Alabama (h00v03 and h01v03) showed the poorest performance. To improve model performance, other AOD products from other algorithms such as AOD data from Deep Blue algorithm<sup>18</sup> at 10-km resolution can be incorporated which is used for bright surfaces. More studies are needed to determine which factors play a role in the prediction of PM<sub>2.5</sub> using satellite imagery and to further improve the performance.

Compared with the existing studies on the similar area,<sup>19–21</sup> our study shows higher  $R^2$  and less errors. After predicting PM<sub>2.5</sub> levels at a 10-km resolution for the similar area for the year 2003,<sup>21</sup> Hu et al.<sup>19</sup> examined the feasibility of the 1-km resolution MAIAC AOD data by comparing with the 10-km data. In their study, the performance of the MAIAC AOD data was comparable with the existing MODIS data but showed slightly lower performance. Our study demonstrated the MAIAC AOD can outperform the existing 10-km data by using various approaches on the top of the advantage of the higher resolution. The study resulted in an  $R^2$  of 0.64 and RMSPE of 3.93  $\mu\text{g}/\text{m}^3$  for the MAIAC data in stage 1. In our model, the lowest  $R^2$  in 2003 was 0.72 with a RMSPE 3.51  $\mu\text{g}/\text{m}^3$ . Recently, they expanded their study period for the same area<sup>20</sup> from a single year of 2003 to the multiple years from 2001 to 2010. Our study area covers vast additional areas in the Southeastern US by adding Florida, Mississippi, and the complete parts of other states. Adopting different approaches than their study, our study shows higher  $R^2$  values and lower RMSPE. The total mean of 10-fold cross-validated  $R^2$  was 0.76 compared with the existing study 0.72 and that of RMSPE from our study was 2.74 compared with 3.72  $\mu\text{g}/\text{m}^3$ . Considering that our study area includes the most southern area such as Florida which showed the lowest performance with a big difference and we applied site-based cross-validation rather than observation-based cross-validation which produces higher  $R^2$ , the actual improvement is expected to be bigger.

In conclusion, we have demonstrated that the use of satellite imagery and other land-use variables with a mixed-effect model produces reliable predictions of daily PM<sub>2.5</sub> for the large area of the Southeastern United States. By incorporating land-use terms and spatial smoothing, our models perform much better than previous studies. Therefore, our model results can be used in various epidemiological studies investigating the effects of PM<sub>2.5</sub> allowing one to assess both acute and chronic exposures with the implication of a new application. Our model results will extend the existing studies on PM<sub>2.5</sub> mainly targeted only for urban areas tied

to the lack of monitors into new areas which used not to be studied such as rural areas.

## CONFLICT OF INTEREST

The authors declare no conflict of interest.

## REFERENCES

- Dockery DW, Pope CA, Xu X, Spengler JD, Ware JH, Fay ME et al. An association between air pollution and mortality in six U.S. cities. *N Engl J Med* 1993; **329**: 1753–1759.
- Pope CA 3rd. Epidemiology of fine particulate air pollution and human health: biologic mechanisms and who's at risk? *Environ Health Perspect* 2000; **108**: 713–723.
- Pope CA 3rd, Burnett RT, Thun MJ, Calle EE, Krewski D, Ito K et al. Lung cancer, cardiopulmonary mortality, and long-term exposure to fine particulate air pollution. *JAMA* 2002; **287**: 1132–1141.
- Barnett AG, Williams GM, Schwartz J, Best TL, Neller AH, Petroeschevsky AL et al. The effects of air pollution on hospitalizations for cardiovascular disease in elderly people in Australian and New Zealand cities. *Environ Health Perspect* 2006; **114**: 1018–1023.
- Rhomberg LR, Chandalia JK, Long CM, Goodman JE. Measurement error in environmental epidemiology and the shape of exposure-response curves. *Crit Rev Toxicol* 2011; **41**: 651–671.
- Armstrong BG. Effect of measurement error on epidemiological studies of environmental and occupational exposures. *Occup Environ Med* 1998; **55**: 651–656.
- Goldman GT, Mulholland JA, Russell AG, Strickland MJ, Klein M, Waller LA et al. Impact of exposure measurement error in air pollution epidemiology: effect of error type in time-series studies. *Environ Health* 2011; **10**: 61.
- Ryan PH, LeMasters GK. A review of land-use regression models for characterizing intraurban air pollution exposure. *Inhal Toxicol* 2007; **19**: 127–133.
- de Hoogh K, Wang M, Adam M, Badaloni C, Beelen R, Birk M et al. Development of land use regression models for particle composition in twenty study areas in Europe. *Environ Sci Technol* 2013; **47**: 5778–5786.
- Beckerman BS, Jerrett M, Martin RV, van Donkelaar A, Ross Z, Burnett RT. Application of the deletion/substitution/addition algorithm to selecting land use regression models for interpolating air pollution measurements in California. *Atmos Environ* 2013; **77**: 172–177.
- Wang R, Henderson SB, Sbihi H, Allen RW, Brauer M. Temporal stability of land use regression models for traffic-related air pollution. *Atmos Environ* 2013; **64**: 312–319.
- Whitworth KW, Symanski E, Lai D, Coker AL. Kriged and modeled ambient air levels of benzene in an urban environment: an exposure assessment study. *Environ Health* 2011; **10**: 21.
- Kloog I, Koutrakis P, Coull BA, Lee HJ, Schwartz J. Assessing temporally and spatially resolved PM<sub>2.5</sub> exposures for epidemiological studies using satellite aerosol optical depth measurements. *Atmos Environ* 2011; **45**: 6267–6275.
- Alston EJ, Sokolik IN, Kalashnikova OV. Characterization of atmospheric aerosol in the US Southeast from ground- and space-based measurements over the past decade. *Atmos Meas Tech* 2012; **5**: 1667–1682.
- Lyapustin A, Wang Y, Laszlo I, Kahn R, Korkin S, Remer R et al. Multiangle implementation of atmospheric correction (MAIAC): 2. Aerosol algorithm. *J Geophys Res* 2011; **116**: D03211.
- Lee HJ, Liu Y, Coull BA, Schwartz J, Koutrakis P. A novel calibration approach of MODIS AOD data to predict PM<sub>2.5</sub> concentrations. *Atmos Chem Phys* 2011; **11**: 7991–8002.
- Jin S, Yang L, Danielson P, Homer C, Fry J, Xian G. A comprehensive change detection method for updating the National Land Cover Database to circa 2011. *Remote Sens Environ* 2013; **132**: 159–175.
- Li X, Xia X, Wang S, Mao J, Liu Y. Validation of MODIS and deep blue aerosol optical depth retrievals in an arid/semi-arid region of northwest China. *Particulology* 2012; **10**: 132–139.
- Hu X, Waller LA, Lyapustin A, Wang Y, Al-Hamdan MZ, Crosson WL et al. Estimating ground-level PM<sub>2.5</sub> concentrations in the Southeastern United States using MAIAC AOD retrievals and a two-stage model. *Remote Sens Environ* 2014; **140**: 220–232.
- Hu X, Waller LA, Lyapustin A, Wang Y, Liu Y. 10-year spatial and temporal trends of PM<sub>2.5</sub> concentrations in the southeastern US estimated using high-resolution satellite data. *Atmos Chem Phys* 2014; **14**: 6301–6314.
- Hu X, Waller LA, Al-Hamdan MZ, Crosson WL, Estes SM et al. Estimating ground-level PM<sub>2.5</sub> concentrations in the southeastern U.S. using geographically weighted regression. *Environ Res* 2013; **121**: 1–10.